Brief Communication

Investigation of differential diffusion in turbulent jet flows using planar laser Rayleigh scattering

Robert W. Dibble [a,*], Marshall B. Long [b]

[a] *Department of Mechanical Engineering, University of California at Berkeley, Berkeley, CA 94720, USA*
[b] *Department of Mechanical Engineering, Yale University, New Haven, CT 06520-8284, USA*

1. Introduction

In 1979, Professor Bilger was among the first faculty to have a sabbatical visit at the new Combustion Research Facility (CRF) at Sandia Laboratories, in Livermore, California. During this sabbatical, Professor Bilger received from Dr. Mike Drake, then at General Electric Corporate Research and Development, an advance copy of the pioneering paper of Raman scattering in a turbulent flame of H_2 into air, later published as Drake et al. [1]. Bilger recognized that the laser Raman data were showing the effects of differential diffusion of H_2 relative to diffusion of oxygen, nitrogen, and water. In the turbulent jet flame of H_2, the effects of differential diffusion were convolved with chemical reaction and heat transfer. A seminal paper emerged [2]. Bilger's early interest in differential diffusion led to other experimental [3] and computational [4] investigations of the topic as well.

In an effort to isolate the effect of differential diffusion without the added complication of chemical reaction with heat release, a nonreacting experiment was proposed at the end of the theoretical paper by Bilger and Dibble [5]. That paper presented a numerical model of a turbulent jet of a binary mixture, into air. The binary mixture, henceforth called "fuel," consisted of 7 mol% Freon in 93% H_2. In the numerical model, a turbulent diffusivity was added to the molecular diffusivity of each species, H_2, Freon, and air.

It was predicted that on average, the H_2 would mix faster with the entrained air, with the consequence that at any distance downstream, the radial dispersion of H_2 would be greater than the dispersion of Freon. The turbulent diffusivity increased with Reynolds number, while the molecular diffusivity remained constant, and thus, as Reynolds number increased, the effect of the differential diffusion became increasingly negligible. In an effort to check these predictions, the paper [5] proposed a Rayleigh-scattering experiment that would allow some of the simplifying assumptions to be checked by providing a direct measurement of differential diffusion effects.

In 1982, the Rayleigh-scattering experiment was attempted at the CRF. However, due to limitations of the experimental configuration, the mole ratio of Freon to H_2 could not be held constant to the required precision and the experiment was suspended. Some years later, in 1989, the proposed experiment was accomplished at the CRF with great success. The successful experiment, described below, is essentially the same as that proposed by Bilger and Dibble [5]. Two aspects of the revised experiment were critical to its success. First, a pulsed laser and charge-coupled-device (CCD) imaging detector were used for the measurements instead of a continuous-wave laser and single-point detector. Second, the flow was split into a main turbulent flow and a laminar reference flow, with an additional CCD detector used to ensure that the Rayleigh cross section of the Freon/H_2 mixture was precisely the same as that of air.

One consequence of the (then) new CCD imaging was the novelty of color graphic presentation of

the effects of differential diffusion. These color prints we circulated among many and subsequently several publications on modeling differential diffusion in turbulent nonreactive flows were published. Kerstein and co-workers [6,7] explored the use of linear eddy modeling in capturing differential diffusion. Yeung and Pope [8] explored differential diffusion using direct numerical simulations. As will be seen, the Rayleigh-scattering images showed clearly the effects of differential diffusion, but lacked an absolute concentration. Quantitative measurements of differential diffusion were later accomplished at the CRF by a series of point Raman experiments as presented by Smith et al. [9,10]. Other experimental works dealing with differential diffusion include those by Barlow and Frank [11], Bergmann et al. [12], Long et al. [13], and Meier et al. [14]. These papers in turn stimulated other modeling papers including Kerstein [15], Nislon and Kosaly [16], Kronenburg and Bilger [17], Pitsch and Peters [18], Fox [19], and Pitsch [20]. Despite these and other publications, the basic experimental description and resulting image data are only now being published, in this Short Communication. Experimental measurement of differential diffusion at a lower Reynolds number was presented recently by Brownell and Su [21]. Their findings reinforce the higher Reynolds number results of this paper. In the next section, details of the experimental configuration are given and the experimental results are presented.

2. Experimental configuration

2.1. Flow conditions

Experiments were carried out at the turbulent diffusion flame facility at Sandia National Laboratory in Livermore, California. The main flow consisted of a vertical pipe with exit diameter, d, of 5.3 mm. The pipe was centered within a laminar coflow of filtered

Table 1
Physical properties of the gasses and gas mixtures used

Gas	Molecular weight	Density/ density air	Relative Rayleigh cross section	Mixture mole fractions
H_2	2.02	0.070	0.219	–
Freon 22 ($CHClF_2$)	86.47	2.997	11.591	–
Air	28.85	1.000	0.984	–
Freon/H_2	–	0.267	0.984	0.067/0.933

Rayleigh cross sections are relative to that of N_2.

air. This facility has been used for a variety of experiments in turbulent combustion and mixing [22]. In the experiment, a fuel mixture of Freon 22 ($CHClF_2$) and H_2 was generated with a ratio of Freon/H_2 that caused the Rayleigh cross section of the mixture to be equal to that of air.

Some of the physical properties of the gases used in the experiment are given in Table 1. Precise metering of the gases was done using mass-flow controllers. The Freon/H_2 mixture was split and directed to two separate nozzles—one, the main turbulent jet, and a second, a laminar reference flow. By monitoring the Rayleigh scattering from the ambient air and the potential core of the reference flow, it was possible to ensure that the Rayleigh-scattering cross sections were precisely matched. This feedback control of the experiment was essential to eliminate long-term drift in the flow-metering system and to allow collection of enough data to provide a statistical characterization of the differential diffusion.

2.2. Optical configuration

The experimental configuration used to measure differential diffusion effects is shown schematically in Fig. 1. A sheet of laser light was focused to intersect both the reference flow and the turbulent jet as shown in the figure. The Rayleigh-scattered light from each
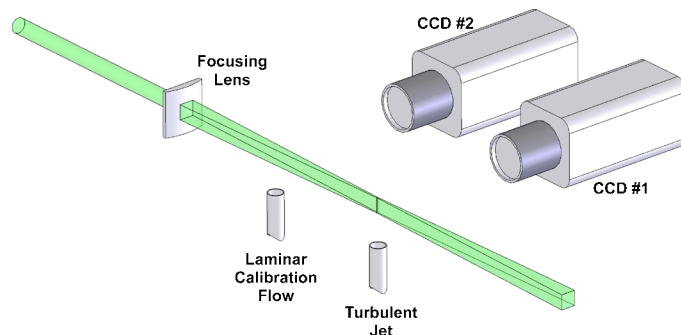
Fig. 1. Experimental setup for measuring differential diffusion in a turbulent jet. A laser beam (focused into either a sheet or a line) intersects both a laminar calibration flow and a turbulent jet. The Rayleigh scattering from each flow is imaged onto a separate cooled CCD detector.

flow was detected normal to the laser sheet by two similar sets of apparatus. For each flow, the scattered light was collected by a pair of camera lenses and imaged onto a separate CCD array detector. The detectors were cooled, slow-scan CCD detectors (Photometrics CC200) with 384×576 pixels (pixel size 20×20 μm^2). Camera controllers associated with the CCD detectors (Photometrics CC220) performed a 14-bit per pixel analog-to-digital conversion and stored the image data until it could be transferred to the microcomputer that controlled the experiment.

A flashlamp-pumped dye laser (the DIANA facility laser at the Sandia Combustion Research Facility) was used in the imaging experiments. This laser provided 0.5 J of energy at 500 nm in a 1.8-μs pulse. The beam was formed into a sheet using cylindrical optics. The 7-mm-high sheet was estimated to be 200 μm thick in the imaged region. (The estimate was made by replacing the cylindrical lens with a spherical lens of the same focal length and measuring the thickness of the resulting beam from the CCD image.)

Fig. 2 shows an example of the Rayleigh intensity recorded by the CCD detector imaging the laminar reference flow and ambient air. On the left of the intensity plot, the Rayleigh signal is from the ambient air, while on the right, the scattering is from the mixture of heavy and light gases (Freon and H_2 for the case shown). At the interface between the two regions (i.e., near the edge of the nozzle), changes in the signal due to differential diffusion are seen with Freon-rich (or equally, H_2-lean) regions scattering more and H_2-rich regions scattering less. The centerline is located on the right of the image, as shown.

The measurement sequence was as follows: (1) mechanical shutters in front of the detectors were opened and the laser-triggered, (2) camera shutters were closed and images read into the camera controllers, (3) the image from the reference flow was transferred to the computer and corrections for background and response were performed, and (4) the ratio of the signal from air and the nozzle gas mixture was obtained. If the ratio was within preset bounds (± 0.5–1.0%) the images from both detectors were recorded. Otherwise, the images were discarded and the sequence repeated. Once the flow metering was set properly, the ratio tended to stay within the bounds for periods of many minutes. However, in the time required to record 600 images, minor adjustments to the flow rates were usually required. The raw images were corrected for nonzero background and response nonuniformities. The same basic experimental configuration was used to obtain a series of line-imaging results. Statistics from the line images were used for comparison with modeling done by Kerstein and co-workers [6,7,15] and will not be discussed further here.
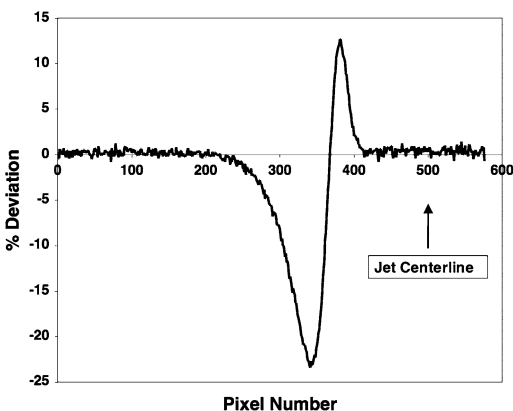
3. Experimental results

Imaging experiments were performed at a variety of downstream locations and at different Reynolds numbers. Representative Rayleigh images are shown for Reynolds numbers (based on nozzle diameter) of 5800, 8600, and 19,000 in Figs. 3, 4, and 5, respectively. Each figure shows images from four different downstream locations, with the downstream location of the imaged regions shown schematically on the left of the figure. The false-color images show the deviation of the Rayleigh signal from that of pure air. Black regions correspond to areas where the Rayleigh signal is the same as that of the ambient air. Orange regions correspond to areas with greater Rayleigh intensity (i.e., Freon-rich regions) and blue corresponds to H_2-rich areas that produce less Rayleigh scattering. The linear color bar to the right of each image indicates the percentage deviation of the signal from that of pure air. To the right of each Rayleigh image shown in Figs. 3–5, the deviation of the Rayleigh signal across the center of the image is shown.

For the imaging experiments, pixels were binned 2×2 to increase the signal/noise, which was 170 in the air coflow after binning. The area projected onto each binned pixel was 75×75 μm^2; the imaged region was $4.0d$ by $1.2d$. Despite being done more than 15 years ago, the signal/noise of this image data compares very favorably with data being published today [23].

4. Discussion

The experiment shows that the effect of differential diffusion is readily observable. Measurable dif-

Fig. 2. The Rayleigh intensity from the laminar reference flow.
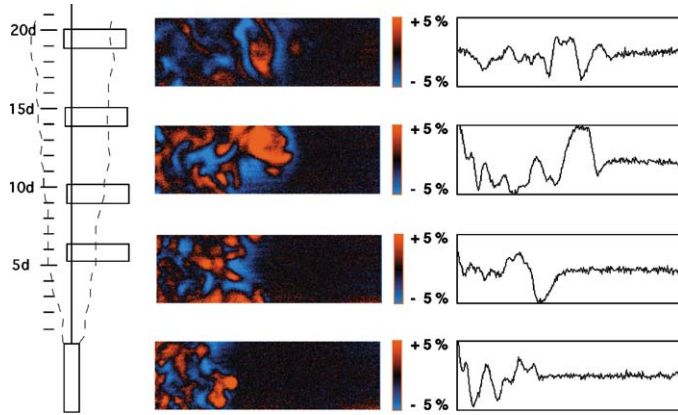
Fig. 3. Rayleigh-scattering images at four different downstream locations in a turbulent Freon/H_2 jet of Re = 5800. The deviation in the plotted Rayleigh intensity from that of air is due to differential molecular diffusion. In the four instantaneous images on the left, the color scale is selected so that black corresponds to the Rayleigh signal from pure air or regions with no differential diffusion. Orange corresponds to regions with a Rayleigh signal slightly larger than that of air, caused by an excess of Freon. Blue regions have an excess of H_2 and, therefore, a smaller Rayleigh signal. The imaged region is 4.0d by 1.2d, with $d = 5.3$ mm the diameter of the axisymmetric nozzle. On the right of the figure, the deviation of the Rayleigh intensity from that of pure air as a function of distance across the center of the image is plotted. The maximum deviations in Rayleigh intensity are on the order of ±5%.
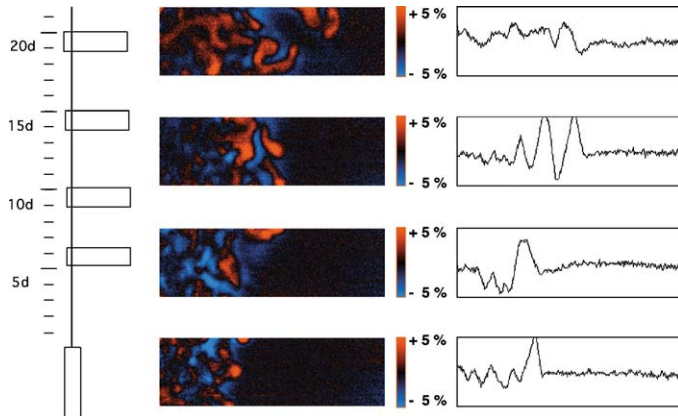
Fig. 4. Rayleigh-scattering images at four different downstream locations in a turbulent Freon/H_2 jet of Re = 8600.
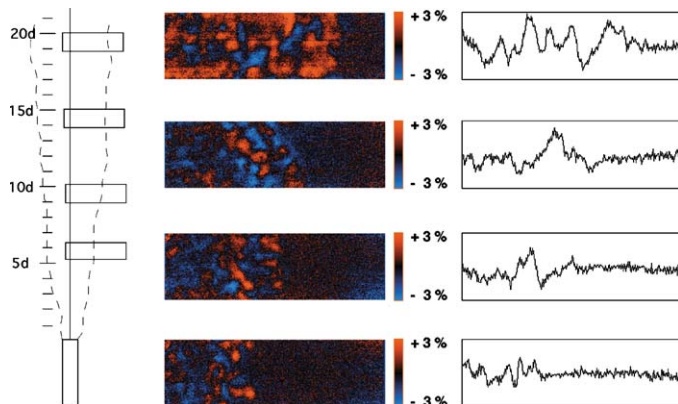
Fig. 5. Rayleigh-scattering images at four different downstream locations in a turbulent Freon/H_2 jet of Re = 19,000.

ferential diffusion is found at Reynolds numbers as high as 20,000 and as far downstream as 30 nozzle diameters. Differential diffusion was observed for both Freon/H_2 and CH_4/H_2 mixtures issued from the nozzle. The images from CH_4/H_2 are not shown, in the interest of brevity, as they echo the images of Freon/H_2.

It should be noted that although the Rayleigh intensity clearly shows all regions in which differential diffusion has occurred, it does not give the mole fraction of the three components (air, Freon, and H_2). However, numerical modeling does predict the mole fractions and these mole fractions can be weighted by the aforementioned Rayleigh-scattering cross sections (see Table 1) to generate images of Rayleigh scattering or statistics such as the mean and rms of Rayleigh-scattered light, as was done by Bilger and Dibble [5]. It is remarkable that to within the accuracy of the measurements, the ensemble average of images produces no net differential diffusion. This is consistent with the point measurements of Smith et al. [10] and not consistent with the average net differential diffusion predicted by Bilger and Dibble [5].

Despite this net effect of differential diffusion, one should not assume that differential diffusion can be ignored. Chemical reactions occur at the interfaces—for example, production of the important pollutant nitric oxide. The instantaneous changes of the chemical environment at the interface, caused by differential diffusion, will lead to changes in product formation that undoubtedly will not be well predicted by models that ignore differential diffusion. In addition, the heat release with combustion causes an increase in transport properties, viscosity, and diffusivity as well as dilatation resulting in slowing down of the rotation of eddies, a consequence of conservation of angular momentum. Thus, the Reynolds number is reduced in combustion flows. Accordingly, we anticipate that models of turbulent combustion that account for differential diffusion at fuel/air interfaces will be more robust. As another example, the role of differential diffusion in stabilizing highly diluted turbulent flames near blowout has also been reported [24].

This experiment illuminated the effects of differential molecular diffusion between species in a nonreacting, isothermal flow. The fuel used in this paper could be burned and explored by Rayleigh thermometry [25,26]. Furthermore, an analogous experiment that explored the effects of thermal diffusivity compared to mass diffusivity could be accomplished by preheating a methane jet so that upon exit from the fuel nozzle, the heated, lower density methane has the same Rayleigh-scattering intensity as the (nonheated) air around it. As the methane turbulently mixed with air, there will be simultaneous heat and mass trans-

fer. If these do not diffuse together, images similar to those shown in this paper are expected to emerge.

5. Conclusion

A series of laser Rayleigh-scattering experiments has been performed to investigate the effects of differential molecular diffusion in turbulent nonreacting jet flows. A turbulent jet of a mixture of Freon and H_2 exiting into coflowing air was studied at various Reynolds numbers. In laminar flow, Rayleigh scattering clearly showed H_2 diffusing ahead of Freon. In turbulent flow, the instantaneous Rayleigh images showed differential diffusion at the many interfaces between jet fluid and entrained air. Yet, ensemble averages of instantaneous images showed no average diffusion of H_2 ahead of Freon.

References

[1] M.C. Drake, M. Lapp, C.M. Penney, S. Warshaw, B.W. Gerhold, Proc. Combust. Inst. 18 (1981) 1521–1531.

[2] R.W. Bilger, AIAA J. 20 (1981) 962–970.

[3] S.H. Stårner, R.W. Bilger, Differential Diffusion Effects on Measurements in Turbulent Diffusion Flames by the Lorenz–Mie Scattering Technique, 1983.

[4] B.M. Lee, H.D. Shin, Combust. Sci. Technol. 62 (1988) 311–330.

[5] R.W. Bilger, R.W. Dibble, Combust. Sci. Technol. 28 (1982) 161–172.

[6] A.R. Kerstein, R.W. Dibble, M.B. Long, B. Yip, K. Lyons, in: Proc. 7th Symposium on Turbulent Shear Flows, Stanford University, August 21–23, 1989, pp. 14.2.1–14.2.6.

[7] R.W. Dibble, A.R. Kerstein, M.B. Long, B. Yip, in: T. Takeno (Ed.), Turbulence and Molecular Processes in Combustion, Elsevier Science, Amsterdam, 1993, pp. 303–310.

[8] P.K. Yeung, S.B. Pope, Phys. Fluids A 5 (1993) 2467.

[9] L.L. Smith, R.W. Dibble, L. Talbot, R.S. Barlow, C.D. Carter, Combust. Flame 100 (1995) 153–160.

[10] L.L. Smith, R.W. Dibble, L. Talbot, R.S. Barlow, C.D. Carter, Phys. Fluids 7 (1995) 1455–1466.

[11] R.S. Barlow, J.H. Frank, Proc. Combust. Inst. 27 (1998) 1087–1095.

[12] V. Bergmann, W. Meier, D. Wolff, W. Stricker, Appl. Phys. B 66 (1998) 489–502.

[13] M.B. Long, S.H. Stårner, R.W. Bilger, Combust. Sci. Technol. 92 (1993) 209.

[14] W. Meier, S. Prucker, M.H. Cao, W. Stricker, Combust. Sci. Technol. 118 (1996) 293–312.

[15] A.R. Kerstein, J. Fluid Mech. 216 (1990) 411–435.

[16] V. Nislon, G. Kosaly, Phys. Fluids 9 (1997) 3386–3397.

[17] A. Kronenburg, R.W. Bilger, Phys. Fluids A 5 (1997) 1435.

[18] H. Pitsch, N. Peters, Combust. Flame 114 (1998) 26–40.

[19] R.O. Fox, Phys. Fluids 11 (1999) 1550.

[20] H. Pitsch, Combust. Flame 123 (2000) 358–374.

[21] C.J. Brownell, L.K. Su, presented at 34th AIAA Fluid Dynamics Conference, Portland, OR, July 2004, paper AIAA 2004-2335.

[22] A.R. Masri, R.W. Dibble, R.S. Barlow, Prog. Energy Combust. Sci. 22 (1996) 307–362.

[23] J.H. Frank, S.A. Kaiser, M.B. Long, Combust. Flame 143 (2005) 507–523.

[24] M.M. Tacke, S. Linow, S. Geiss, E.P. Hassel, J. Janicka, J.Y. Chen, Proc. Combust. Inst. 27 (1998) 1139–1148.

[25] R.W. Dibble, R.E. Hollenbach, Proc. Combust. Inst. 18 (1981) 1489–1499.

[26] D.C. Fourguette, R.M. Zurn, M.B. Long, Combust. Sci. Technol. 44 (1985) 307.